Brain Structure and Function (2022) 227:2957–2969
https://doi.org/10.1007/s00429-022-02554-2

ORIGINAL ARTICLE

Network synchronization deficits caused by dementia and Alzheimer's disease serve as topographical biomarkers: a pilot study

Mohammad Javad Sedghizadeh[1] · Hamid Aghajan[1] · Zahra Vahabi[2,3] · Seyyedeh Nahaleh Fatemi[1] · Arshia Afzal[1]

Received: 1 December 2021 / Accepted: 9 August 2022 / Published online: 23 August 2022

Abstract

Mild cognitive impairment (MCI) is known as an early stage of cognitive decline. Amnestic MCI (aMCI) is considered as the preliminary stage of dementia which may progress to Alzheimer's disease (AD). While some aMCI patients may stay in this condition for years, others might develop dementia associated with AD. Early detection of MCI allows for potential treatments to prevent or decelerate the process of developing dementia. Standard methods of diagnosing MCI and AD employ structural (imaging), behavioral (cognitive tests), and genetic or molecular (blood or CSF tests) techniques. Our study proposes network-level neural synchronization parameters as topographical markers for diagnosing aMCI and AD. We conducted a pilot study based on EEG data recorded during an olfactory task from a group of elderly participants consisting of healthy individuals and patients of aMCI and AD to assess the value of different indicators of network-level phase and amplitude synchronization in differentiating the three groups. Significant differences were observed in the percent phase locking value, theta-gamma phase-amplitude coupling, and amplitude coherence between the groups, and classifiers were developed to differentiate the three groups based on these parameters. The observed differences in these indicators of network-level functionality of the brain can help explain the underlying processes involved in aMCI and AD.

Keywords Neural synchronization deficit · Alzheimer's disease · Topographical biomarker · Olfactory stimulation · Mild cognitive impairment · Electroencephalogram

Introduction

Neural synchronization refers to the simultaneous activity of neuronal groups in the brain. Repetitive spiking activities of neural populations form an oscillatory behavior at frequency ranges from slow delta waves (0.5–3 Hz) to fast gamma waves (> 30 Hz) which can be different from the firing rates of single neurons (Timofeev et al. 2012). Neural synchronization is known to play a role in communication between different regions of the brain (Bonnefond et al. 2017), as well as being involved in the brain's high order processes such as attention (Womelsdorf and Fries 2007), working memory (Reinhart and Nguyen 2019), and consciousness (Valencia and Froese 2020). In the process of neurodegenerative disorders such as Alzheimer's disease (AD), synchronization between brain's neuronal networks is disrupted (Aron and Yankner 2016; Sedghizadeh et al. 2020). This deficiency is also observed in other brain disorders (Babiloni et al. 2020; Quiñones-Camacho et al. 2021) in the form of hyper-synchronization or de-synchronization, and may occur in different oscillatory bands. We refer to this dysfunction as neural synchronization deficit (NSD).

The current study proposes a method based on employing effective indicators of NSD which can serve as biomarkers for detecting AD in its early stage and differentiate AD patients from individuals suffering from mild cognitive impairment (MCI). We assess the possibility of using the brain synchronization parameters in response to olfactory stimulation to derive topographical markers for AD and MCI. Beta-amyloid ($A\beta$) deposition has been reported to occur in early stages of AD in the medial temporal lobe (Mattsson et al. 2019), which contains neural paths involved

✉ Hamid Aghajan
aghajan@ee.sharif.edu

[1] Department of Electrical Engineering, Sharif University of Technology, Tehran, Iran

[2] Department of Geriatric Medicine, Ziaeian Hospital, Tehran University of Medical Sciences, Tehran, Iran

[3] Memory and Behavioral Neurology Division, Roozbeh Hospital, Tehran University of Medical Sciences, Tehran, Iran

in olfactory processing. Several studies have suggested olfactory deficit as a biomarker for the early diagnosis of AD (Talamo et al. 1989; Mesholam et al. 1998), and for predicting the progress of MCI to AD (Devanand et al. 2000). The perception of odors has been reported to be impaired due to AD (Silva et al. 2018; Zou et al. 2016; Sedghizadeh et al. 2020), and the olfactory bulb circuitry projects through the hippocampus and amygdala (Mouly and Sullivan 2010) which are reported to be affected by AD. Moreover, deficit in spatial synchronization in the beta and gamma oscillatory activity in response to olfactory stimulation has been reported as a biomarker for early stages of AD (Sedghizadeh et al. 2020).

We conducted a pilot study on a group of elderly participants with mild AD, amnestic MCI (aMCI), or normal aging conditions to characterize the quality of the brain's oscillations in response to olfactory stimulation, aiming to extend the neurophysiological understanding of these disorders and to derive topographical markers related to deficit in the olfactory function which could help with early detection of AD and aMCI.

Microglia are the principal immunity cells in the central nervous system (CNS). In the process of phagocytosis, the microglia cells engulf external particles and become loaded with non-reactive cells (Galloway et al. 2019). Dysfunction of microglia cells is reported to play a significant role in diseases associated with brain infection, stroke, and dementia (Augusto-Oliveira et al. 2019). The effect of microglia in controlling the $A\beta$ load in the brain (Lee and Landreth 2010) and their functional deficit being associated with AD make them potential players in the progress of the disease.

Rhythmic auditory or visual stimulation can induce oscillations in the brain and synchronize the brain networks at the entrained frequency (Aron and Yankner 2016; Henao et al. 2020). The effect of inducing synchronized oscillations in the brain through sensory entrainment (particularly in the gamma band) on the structural and functional health of microglia has been reported (Iaccarino et al. 2016). The study reported that after inducing gamma oscillations in the brain of mice models of AD, the expression of genes that have a role in the function of microglia was significantly increased.

Inducing synchronized oscillatory activity in the brain by external gamma stimulation has also been reported for the treatment of stroke in a recent study (Balbi et al. 2021), in which synchronized neural activity was improved due to entrainment while morphological enhancements were not observed in microglia cells. While it is still premature to point to concrete differences between the cellular and synaptic mechanisms in AD and stroke that are involved in the oscillatory activity across brain networks based on these studies, the causal effect of microglial dysfunction established for AD can help explain the synchronization deficits caused by AD. Morphological changes and gene expression variations in microglia have been linked to neurodegenerative brain disorders and are reported to cause a deficit in synaptic pruning which leads to decreased functional connectivity (Zhan et al. 2014). Other recent results also suggest that microglia have significant effect on synaptic sculpting (Liu et al. 2021) and in the preservation of neuronal connectivity (Jebelli et al. 2015). According to these studies, the interaction between microglia and synapses controls the neural activity and synchronization of the local neuronal population (Akiyoshi 2018). Hence, while more studies are needed to reveal and interpret the direct link between NSD and AD and the potential cycles of cause and effect involved in the progress of the disease, reported studies on the role of microglia deficit in AD on the one hand, and other reports that link microglia dysfunction to NSD on the other, may help inform the processes that lead to the large-scale and network-level synchronization deficit as a manifest of synaptic changes that are caused by $A\beta$ accumulation.

MCI is known as a cognitive state between normal aging and dementia due to AD. It is a heterogeneous clinical concept that can point to various underlying reasons or diseases (Petersen 2016). There are two clinical types of MCI: amnestic (aMCI) and non-amnestic (naMCI). Amnestic MCI is considered as the preliminary stage of cognitive impairment due to Alzheimer's disease (Petersen 2016) and is more likely to progress to AD compared to naMCI (Jungwirth et al. 2012). Cognitive deficits in aMCI may include impairment in learning and recall of recent information, with impairment in at least one other domain such as reasoning or completing complex tasks, visuospatial abilities, language functions and behavior. While some aMCI patients may stay in this condition for years, others might develop dementia associated with AD (Albert et al. 2011). Early detection of aMCI allows for potential treatments to prevent or decelerate the process of developing dementia (Hahn and Andel 2011).

According to (Dubois et al. 2014), topographical markers identify downstream brain changes associated with the AD pathology, such as subsequent cognitive and behavioral changes. Even though these markers may lack pathological specificity for AD, they might be particularly valuable in the diagnosis of the disease and monitoring its progress (Dubois et al. 2014). To examine the various indicators of synchronized neural activity reflecting NSD in the brain which can potentially serve as topographical biomarkers for aMCI and AD, we extract different temporal and spatial synchronization indicators from EEG data recorded in an olfactory oddball task.

Previous studies have analyzed Event-Related Potentials (ERP) and functional brain connectivity during auditory, visual, or olfactory oddball tasks. In Caravaglios (2010), it was suggested that the change in the theta power after stimulation during an oddball auditory task is significantly higher

Table 1 Demographic information of participants

Characteristic	Healthy ($n=15$)	AD ($n=13$)	aMCI ($n=7$)	p value		
				Healthy-aMCI	Healthy-AD	aMCI-AD
Age (years)	69.27 ± 6.65	75.31 ± 9.90	66.57 ± 6.85	0.391	0.066	0.053
Gender, % female	%53.33	%61.54	%51.14	0.875	0.676	0.858
Education (years)	4.93 ± 4.70	3.31 ± 2.95	5.86 ± 6.77	0.713	0.292	0.252
MMSE score	25.73 ± 3.20	16.46 ± 3.20	23.71 ± 2.93	0.172	4.075E−08	9.983E−05

Mean value and standard deviation of each demographic feature for healthy individuals and AD and aMCI patients are listed

in healthy individuals compared to AD patients. Another study (Güntekin et al. 2008) reported that the coherence of the evoked theta band during a visual oddball task was significantly higher across the frontal-parietal channel pairs in healthy controls than in AD patients. The theta phase-locking value following deviant stimulation in a visual oddball task was also shown in another study (Yener et al. 2007) to be significantly higher in healthy controls and AD patients treated with cholinesterase inhibitors compared to non-treated AD patients. Cross-frequency coupling patterns and auditory eventrelated potentials (AERP) were studied in aMCI patients during an active counting auditory oddball task and the quality of the cross-frequency coupling was found to be correlated with the performance in the cognitive task (Dimitriadis et al. 2015).

In the following sections of the paper, we first describe our experimental protocol for olfactory stimulation in the Methods section. This section also includes the mathematical derivations of a number of indicators linked to NSD which are extracted from EEG data in our study. In the Results section, we present the results of monitoring these indicators between three groups of healthy controls and patients of aMCI and AD, and integrate the various indicators representing temporal and spatial synchronization deficit into a flowchart which can be employed as an NSD-based topographical biomarker to reliably differentiate the three groups of participants. The section Discussion and Limitations summarizes our findings and describes the limitations of the current study.

Methods

Participants

This study was approved by the Review Board of Tehran University of Medical Sciences (Approval ID: IR.TUMS.MEDICINE.REC.1398.524). All methods were performed in accordance with the relevant guidelines and regulations, and all participants gave their written consent before beginning the experiment. The name and date of birth of the participants were kept confidential and were not used in any of the analyses. The experiment was carried out at the Department of Geriatric Medicine of Ziaeian Hospital, under the supervision of two expert neuropsychologists.

A total of 44 participants including aMCI and AD patients and healthy (normal) individuals were recruited for this study. Six participants were removed from the study prior to conducting the experiments due to a history of stroke, brain injury, or olfactory system dysfunction. Other participants diagnosed with Parkinson's disease, multi-system atrophy, and other neurodegenerative diseases (other than dementia and AD) were also excluded from the study. Given these selection criteria, 35 participants remained (age = 70.97 ± 8.58, female = 57.14%) which included 15 healthy (normal) individuals (age = 69.27 ± 6.65, female = 53.33%), and 7 aMCI (age = 66.57 ± 6.85, female = 51.14%) and 13 AD (age = 75.31 ± 9.90, female = 61.54%) patients. Given a statistical power of 95% and a 5% type I error, at least seven participants were required for each group to allow for a statistically valid comparison between the normal, aMCI, and AD participants. Table 1 shows the demographic information of the participants.

Prior to the experiment, a mini-mental state examination (MMSE) test, clock drawing test (CDT), and a verbal fluency test were performed by a neurologist to assess the cognitive state of the participants. MMSE is a 30-point test which assesses different cognitive functions such as attention, memory, orientation and language, and allows for the evaluation of cognitive impairment. The MMSE detailed results are shown in Table 2 along with the age range and diagnosed mental state of the participants. The mental states of the participants were diagnosed by the neurologist based on these tests as well as structural MRI

Table 2 MMSE scores of the participants and their mental state

Subject Number	Mental State	Age	O place	O time	Reg	Att & Calc	Naming	Rep	Read	Write	DR	VS	Comm	Total MMSE
1	Normal	65–70	5	5	3	**5**	2	1	**1**	**1**	3	1	3	30
2	Normal	70–75	5	5	3	**1**	2	1	**0**	**0**	2	0	3	21
3	Normal	60–65	5	5	3	**5**	2	1	**1**	**1**	2	1	3	29
4	Normal	65–70	5	5	3	**1**	2	1	**0**	**0**	1	0	3	21
5	Normal	75–80	5	5	3	**4**	2	1	**1**	**0**	2	1	3	27
6	Normal	70–75	5	5	3	**3**	2	1	**1**	**1**	2	1	3	28
7	Normal	55–60	5	5	3	**2**	2	1	**1**	**1**	3	1	3	27
8	Normal	75–80	5	4	3	**4**	2	1	**0**	**0**	2	0	3	23
9	Normal	75–80	5	4	3	**3**	2	1	**1**	**1**	2	0	3	26
10	Normal	70–75	5	5	3	**5**	2	1	**1**	**1**	3	1	3	30
11	Normal	65–70	5	5	3	**4**	2	0	**1**	**0**	2	1	3	26
12	Normal	60–65	5	5	3	**3**	2	1	**1**	**1**	3	1	3	28
13	Normal	75–80	5	4	3	**4**	2	1	**0**	**0**	2	0	3	23
14	Normal	70–75	4	5	3	**2**	2	1	**1**	**1**	3	1	3	26
15	Normal	65–70	4	5	3	**1**	2	0	**0**	**0**	3	0	3	21
16	aMCI	55–60	4	4	3	**4**	2	0	**0**	**0**	2	0	3	22
17	aMCI	70–75	4	4	3	**3**	2	0	**0**	**1**	2	0	3	22
18	aMCI	60–65	5	4	3	**1**	1	0	**1**	**1**	2	0	3	21
19	aMCI	70–75	5	3	3	**3**	2	0	**0**	**3**	1	0	3	21
20	aMCI	70–75	5	5	3	**3**	2	1	**1**	**1**	1	0	3	25
21	aMCI	60–65	5	5	3	**4**	2	1	**1**	**1**	2	0	3	27
22	aMCI	70–75	5	5	3	**4**	2	1	**1**	**1**	2	1	3	28
23	AD	80–85	5	4	3	**1**	2	0	**0**	**0**	0	0	3	18
24	AD	75–80	4	4	3	**0**	2	1	**1**	**1**	0	1	2	19
25	AD	70–75	5	2	3	**0**	2	0	**0**	**0**	0	0	3	15
26	AD	65–70	2	3	3	**0**	2	0	**0**	**0**	0	0	2	12
27	AD	75–80	5	2	3	**0**	2	1	**0**	**0**	2	0	1	16
28	AD	70–75	3	5	3	**3**	2	0	**1**	**1**	0	0	1	19
29	AD	80–85	5	2	3	**0**	2	0	**1**	**1**	0	0	3	17
30	AD	60–65	2	3	3	**0**	2	0	**0**	**0**	0	0	3	11
31	AD	85–90	4	3	3	**0**	2	1	**0**	**0**	0	0	3	16
32	AD	85–90	3	2	3	**0**	2	1	**0**	**0**	0	0	2	12
33	AD	55–60	5	2	3	**2**	2	1	**0**	**0**	2	0	3	20
34	AD	65–70	3	2	3	**0**	2	1	**0**	**0**	3	0	3	18
35	AD	75–80	4	2	3	**3**	2	1	**1**	**1**	0	1	3	21

The table shows each participant's age as a range, their diagnosed mental state, and the details of their MMSE score. *O Time* Orientation to time, *O Place* Orientation to Place, *Reg* Registration, *Att & Calc* Attention and Calculation, *DR* Delayed Recall, *Rep* Repetition, *VS* Visuospatial, *Comm* Commands. The bold columns are components of the test that have dependence on the literacy of the participants

data. It is noteworthy to mention that the participants were classified based on their MMSE scores considering their level of education. This literacy level-based adjustment is necessary due to the fact that some of the questions of the test (Attention and Calculation, Read, and Write; see Table 2) correlate with the literacy level of the participants, and hence a lower value compared to the usual score threshold may be used by the neurologist to classify the participants with very low literacy levels (see participant numbers 2, 4, and 15 in Table 2 as examples).

Task description

Participants performed an oddball olfactory task which consisted of 120 trials, each composed of 2 s of olfactory stimulation followed by 8 s of rest. The entire experiment took about 20 min for each participant. Odors were presented in a pre-set randomized order, lemon being the standard (frequent) odor presented with a probability of 0.75 and rose as the deviant (non-frequent) odor with a probability of 0.25. Pure water was presented as the neutral odor during rest.

The presentation of odors was performed using a computer-controlled olfactometer described in (Hojjati et al. 2019).

EEG data acquisition and preprocessing

EEG data were acquired during the task using a 19-channel standard 10–20 system. Data were referenced to A1 and A2 due to the minimal electrical activity in these electrodes. The impedance of the electrodes was kept under 15 kΩ during the experiment. The sampling frequency was set to 2000 Hz, and was later reduced to 200 Hz through filtering and subsampling.

All preprocessing was performed using MATLAB 2018b and EEGLab v2021.0 (Delorme and Makeig 2004). The data were filtered from 0.5 to 45 Hz using a bandpass filter and epoched from 1 s pre-stimulus to 2 s post-stimulus. Artifacts were removed by running independent component analysis (ICA) using the logistic infomax ICA algorithm (Bell and Sejnowski 1995). A maximum of one artifactual component was identified as "Muscle", "Heart", "Eye", or "Other" by EEGLab, which was removed and only the components labeled as "Brain" were kept for further analysis.

Noisy trials were identified by eye and were removed from further analysis. Following the methods reported in earlier studies (Morgan and Murphy 2002), only the data of the Fz, Cz, and Pz channels were used for biomarker extraction.

Biomarkers

Different topographical biomarkers were assessed for classifying normal, aMCI, and AD cases. Since deficits in the brain's functional connectivity have been observed in AD patients (Zhao et al. 2020; Wang et al. 2019), different indicators of connectivity and synchronization were studied for developing a classification method. These indicators are described next.

Percent phase locking

AD is associated with deficits in the phase synchronization of gamma oscillations. Several studies have reported on the importance of phase synchronization in the oscillatory gamma activity in performing memory and attention tasks, which is degraded in AD and leads to deficits in memory function (Kramer et al. 2007; Knyazeva et al. 2012; Kleen et al. 2016).

A method based on Shannon entropy has been proposed in (Tass et al. 1998) for assessing the phase locking status of EEG signals. Based on this method, an indicator named percent phase locking (PPL) has been proposed in (Rubino et al. 2006) to quantify the phase locking status of brain signals to a stimulus onset. The measurement of this indicator is described next according to the review article (Liang et al. 2016).

First, the instantaneous phase of the signal is extracted using Hilbert transform and is wrapped to the $[0–2\pi]$ interval, which is divided into N bins. Then, the number of instantaneous phase values that lie within each bin is calculated. Using these values and Shannon entropy, the entropy of the distribution of the instantaneous phase for each trial is calculated:

$$s = -\sum_{k=1}^{N} \frac{m_k}{M} \log\left(\frac{m_k}{M}\right),$$

where m_k is the number of phase samples that lie within the kth bin, and M is the total number of phase samples in a trial. The optimal value of N is set to $e^{0.626+0.4\log(M)}$. In this study, we chose the 0–0.7 s post-stimulus interval since the estimated latency of the olfactory response is known to be between 600 and 700 ms. The phase of gamma oscillations (39–41 Hz) was calculated using Hilbert transform for each non-frequent odor trial on the Fz, Cz, and Pz channels. It should be mentioned that the extracted phase of the signal has valid information only if the signal is narrowband (Le Van Quyen et al. 2001), so we filtered the signal to contain the target oscillations (39–41 Hz) in the gamma band. Choosing the narrowband filter around 40 Hz was based on the importance of the 40 Hz oscillations which are reported to occur during olfactory stimulation (Bouyer et al. 1981; Montaron et al. 1982) and during inhalation and exhalation (Kay 2015).

Then, the value of PPL for each trial was calculated as a percentage value using the following formula:

$$\mathrm{PPL}_n = \frac{\log(N) - s}{\log(N)} \times 100 \text{ (PPL for the } n\text{th trial)}.$$

The total mean of the PPL values over trials was calculated for each channel for each participant. Higher PPL values show higher phase locking to the stimulus onset. The mean and SEM (standard error of the mean) of the resulting PPL values for the three different groups of participants are shown in Fig. 1.

Amplitude coherence

Synchronization of the gamma activity between different regions of the brain is another network-level mechanism that underlies memory and cognition (Jia et al. 2011). Amplitude coherence (Srinath and Ray 2014) is an indicator of spatial synchrony, which quantifies the synchronization of the amplitude fluctuations of two given signals. Amplitude coherence between channels Fz and Cz is defined as follows:

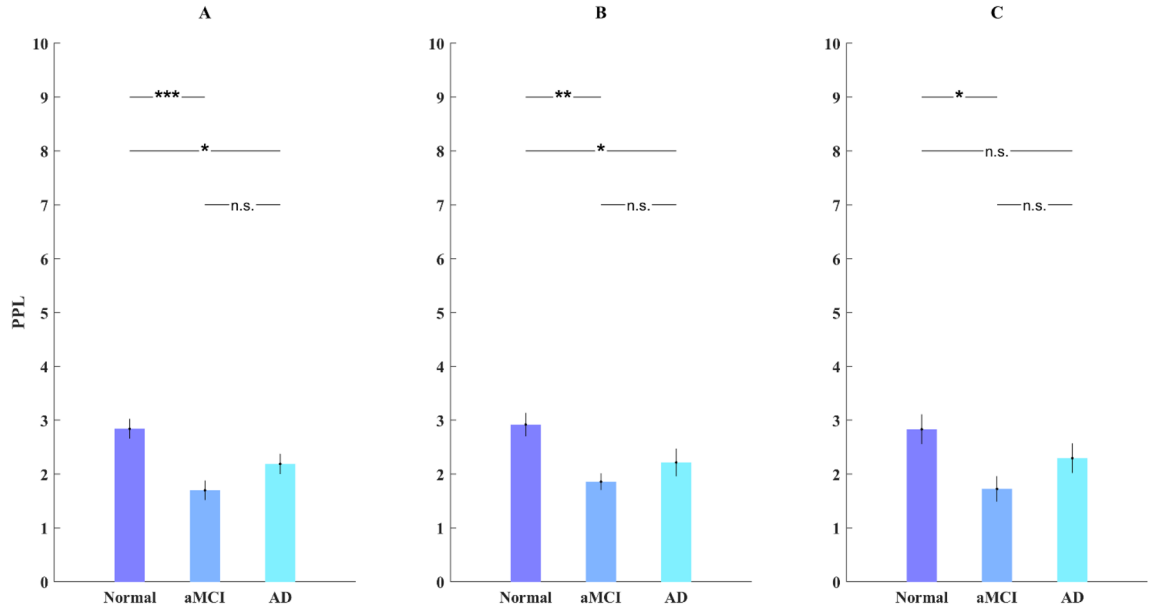

Fig. 1 PPL for healthy controls and aMCI and AD patients. PPL was calculated on channels **A** Fz **B** Cz **C** Pz for the non-frequent odor trials in the frequency range (39-41 Hz) in the gamma band. To assess the phase locking to the stimulus onset, the 0–0.7 s time interval after the stimulus onset was selected in each trial. A significant difference can be seen between the healthy group and the aMCI and AD groups in channels Fz and Cz (ns: not significant; $*p<0.05$; $**p<0.01$; $***p<0.001$. $n=15$ Normal, $n=13$ AD, $n=7$ aMCI were used in this bar plot)

$$C_{\text{amp}}(f)=\left|\frac{\sum_k(A_{k_{\text{Cz}}}(f)-A_{\text{mean}_{\text{Cz}}}(f))(A_{k_{\text{Fz}}}(f)-A_{\text{mean}_{\text{Fz}}}(f))}{\sqrt{\sum_k(A_{k_{\text{Cz}}}(f)-A_{\text{mean}_{\text{Cz}}}(f))^2}\sqrt{\sum_k(A_{k_{\text{Fz}}}(f)-A_{\text{mean}_{\text{Fz}}}(f))^2}}\right|,$$

where k is the number of trials and A_k is the absolute value of the Fast Fourier Transform (FFT) of the data record in each trial.

To calculate amplitude coherence, the 0–1 s post-stimulus interval was used and the slow-gamma oscillations (35–45 Hz) were extracted for each trial. $A_{k_{\text{Cz}}}$ and $A_{k_{\text{Fz}}}$ were calculated for each participant and C_{amp} was calculated for each frequency sample. Next, the values corresponding to the 35–45 Hz frequencies were averaged, yielding a mean C_{amp} value for each participant. The mean and SEM of these values for the three different groups of participants are plotted in Fig. 2.

Theta-gamma phase-amplitude coupling

Phase-amplitude coupling (PAC) of different frequency bands in the brain has been suggested to be involved in the underlying mechanisms for different cognitive functions. Individuals diagnosed with AD show deficits of phase-amplitude coupling in their neural activity (Poza et al. 2017). It has been shown that the phase of slow oscillations in the brain [theta frequency band (4–8 Hz)] modulate the amplitude of higher frequency bands [slow gamma (35–45 Hz)], and that this neural mechanism is involved in performing memory-related tasks (Lega et al. 2014).

Several methods have been proposed for calculating the theta-gamma PAC. We used a recently introduced method called the time–frequency mean vector length (tf-MVL) (Munia and Aviyente 2019a, b). Unlike other methods that use Hilbert transform for extracting the phase of theta oscillations, tf-MVL uses the reduced interference distribution (RID)-Rihaczek method to simultaneously estimate the phase of the slow oscillations and the amplitude of the higher frequency oscillations. This method provides a more accurate estimate of the phase and amplitude of the signal as it does not depend on the parameters of filters to extract the theta and gamma components (Munia and Aviyente 2019a, b).

In this study, we compared the theta-gamma PAC for non-frequent odor trials on the Fz, Cz, and Pz channels. To this end, the data of each channel was normalized as z-score, setting the mean of each channel to zero and its standard deviation to 1. Next, the overall mean of the rest trials for each participant was subtracted from the average trial on each channel. Using the RID-Rihaczek distribution, the phase and amplitude of theta (4–8 Hz) and gamma (39–41 Hz)

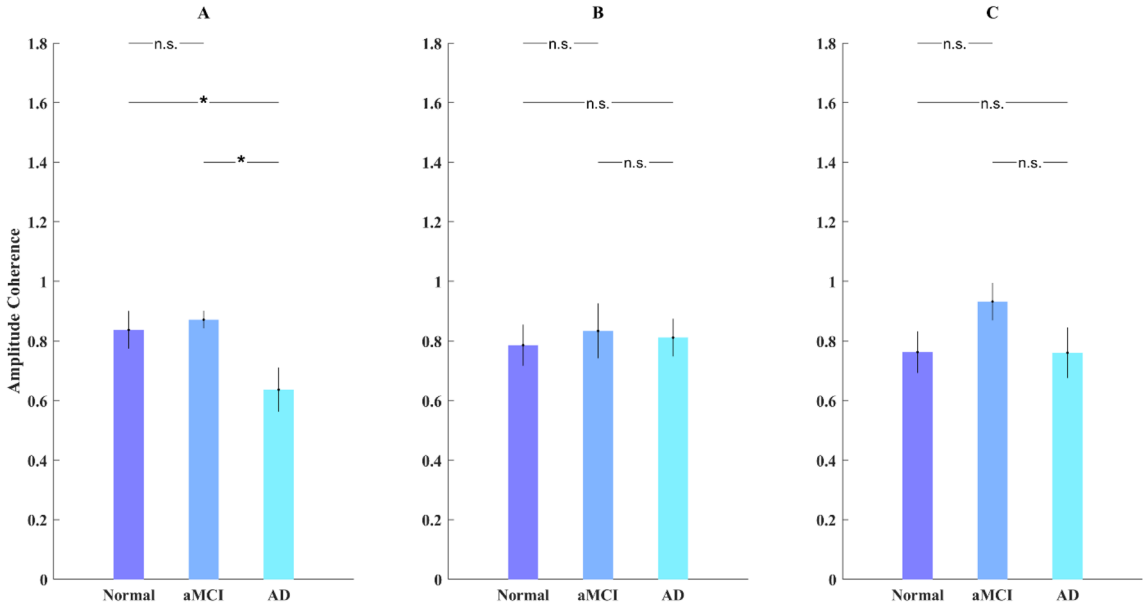

Fig. 2 Amplitude Coherence for healthy controls and aMCI and AD patients. Amplitude coherence was calculated between the **A** Fz–Cz, **B** Fz–Pz, and **C** Cz–Pz channel pairs for the non-frequent odor trials in the frequency range (35–45 Hz) in the gamma band. To measure the amplitude coherence, the 0–1 s time interval after the stimulus onset was selected in each trial. A significant difference can be seen between the AD group and the healthy and aMCI groups in Fz-Cz amplitude coherence (ns: not significant; $*p<0.05$; $**p<0.01$; $***p<0.001$. $n=15$ Normal, $n=13$ AD, $n=7$ aMCI were used in this bar plot)

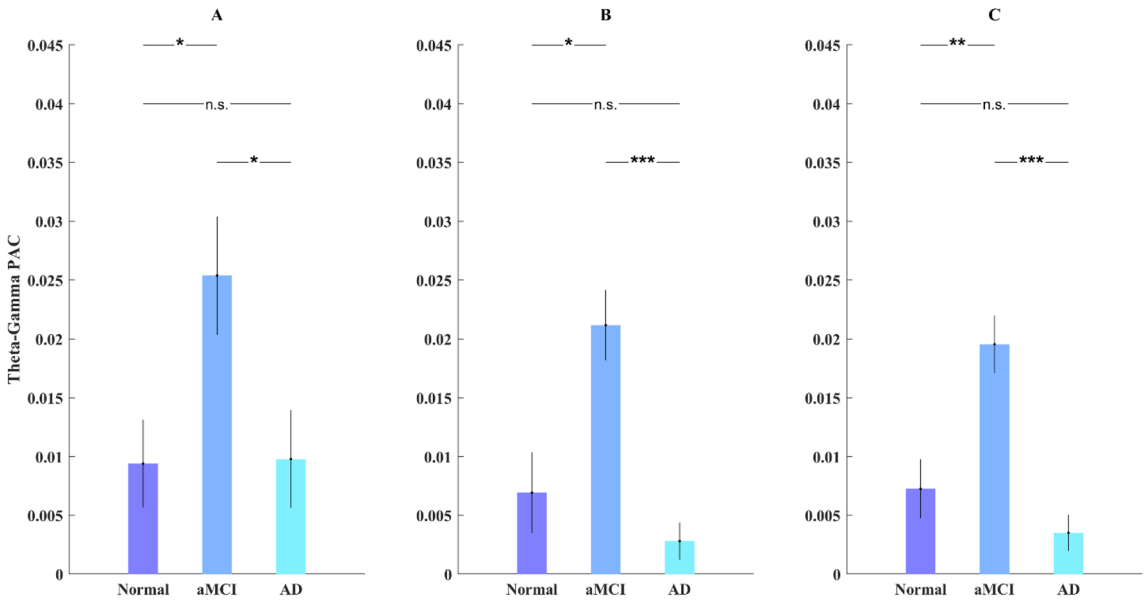

Fig. 3 Theta-Gamma Phase Amplitude Coupling (PAC) for healthy controls and aMCI and AD patients. Theta (4–8 Hz)-gamma (39–41 Hz) PAC was calculated on channels **A** Fz, **B** Cz, and **C** Pz for the 0–2 s time interval after the stimulus onset in the frequent odor trials. A significant difference is observed between the aMCI group and both the healthy and AD groups for all three channels (ns: not significant; $*p<0.05$; $**p<0.01$; $***p<0.001$. $n=15$ Normal, $n=13$ AD, $n=7$ aMCI were used in this bar plot)

oscillations were extracted and the theta-gamma PAC value for each channel was calculated using the following formula:

$$\text{theta} - \text{gamma PAC} = \left| \frac{1}{N} \sum_{i=1}^{N} A_i e^{j\varphi_i} \right|,$$

in which N is the length of the average trial on each channel, A is the amplitude of the sum of all the values corresponding to the slow-gamma frequency band in the (RID)-Rihaczek distribution, and φ is the angle of the sum of the values within the low frequency band in the time–frequency distribution.

The theta-gamma PAC was calculated for each participant and the mean and SEM of these values for channels Fz, Cz, and Pz are plotted in Fig. 3.

Classification

Multiple binary SVM classifiers can be used for classifying data that consists of more than two groups. To classify the three groups of participants, two binary SVM classifiers were trained, both using as input the five features introduced in this section (PPL of channel Cz, amplitude coherence between channels Fz and Cz, and three PAC values for channels Fz, Cz, and Pz). The features were normalized before training the classifiers. One binary SVM classifier was trained for classifying healthy individuals and aMCI patients, and another for classifying aMCI and AD patients. For these two classifications, we separately trained a linear SVM classifier and a nonlinear SVM classifier using a radial basis function (RBF) kernel. While a nonlinear classifier may offer better performance through remapping of the features, using a linear classifier can demonstrate the intrinsic efficacy of the features regardless of the classification method. We also trained two binary Random Forest (RF) classifiers, one for classifying healthy individuals and aMCI patients, and another for classifying aMCI and AD patients.

Since the data used in these classifications were unbalanced, a stratified fivefold cross validation was performed to evaluate the performance of the classifiers. This allows for maintaining a fixed ratio between the number of positive and negative samples in all folds. Using this method, the mean and standard deviation of accuracy, precision, and recall were reported for all SVM and RF classifiers. The design of the classifiers and cross validation methods was conducted using the Python scikit-learn package[1] (Pedregosa et al. 2011).

Statistical analyses

All results are expressed as mean $\pm \frac{\sigma}{\sqrt{n-1}}$, where n is the number of participants for each group, and σ is the standard deviation of the variable of interest. All p values were calculated using two-tailed t tests by MATLAB ttest2 function. Significance levels of 0.05, 0.01, and 0.001 were examined in each comparison.

Results

PPL is significantly higher in healthy participants compared to aMCI and AD patients

We used PPL values to compare the phase locking of gamma oscillations to the stimulus onset in healthy controls and the aMCI and AD patients. Our results show a significantly higher phase-locking value in healthy participants compared to both aMCI and AD patients on channels Fz and Cz (Fig. 1).

Amplitude coherence is significantly lower in AD patients

Amplitude coherence is an indicator of the brain's functional connectivity as it represents the similarity between the amplitude fluctuations of different brain signals, neglecting the effect of the phase of the signals. Our results show that the amplitude coherence values measured between channels Fz and Cz for the AD group are significantly lower compared to the healthy and aMCI groups, whereas the amplitude coherence values between the same two channels are not significantly different between the aMCI and healthy groups (Fig. 2).

Significant difference is observed in theta-gamma phase-amplitude coupling between aMCI patients and both healthy and AD groups

Comparing the theta-gamma PAC values measured at the Fz (Fig. 3A), Cz (Fig. 3B), and Pz (Fig. 3C) channels for the three groups shows significant differences between the aMCI group and both the healthy and AD groups in all three channels. A remarkable observation in the results of all three channels is the relatively higher values of the theta-gamma PAC in aMCI patients compared to both the healthy and AD groups.

[1] https://scikit-learn.org/stable/modules/generated/sklearn.model_selection.StratifiedKFold.html.

Table 3 Detailed classification statistics

Model	Accuracy	Precision	Recall
SVM (RBF kernel)			
2-class SVM (Normal-aMCI)	0.87 ± 0.11	0.83 ± 0.23	0.80 ± 0.19
2-class SVM (AD-aMCI)	0.85 ± 0.12	0.88 ± 0.10	0.87 ± 0.11
Combination of two 2-class SVMs (aMCI-AD + Normal-aMCI)	0.73 ± 0.21	0.73 ± 0.15	0.74 ± 0.19
SVM (linear kernel)			
2-class SVM (Normal-aMCI)	0.91 ± 0.11	0.93 ± 0.10	0.92 ± 0.11
2-class SVM (AD-aMCI)	0.80 ± 0.19	0.78 ± 0.24	0.78 ± 0.24
Combination of two 2-class SVMs (aMCI-AD + Normal-aMCI)	0.64 ± 0.19	0.56 ± 0.24	0.60 ± 0.19
Random forest (RF)			
2-class RF (Normal-aMCI)	0.90 ± 0.20	0.93 ± 0.13	0.93 ± 0.13
2-class RF (AD-aMCI)	0.90 ± 0.12	0.92 ± 0.11	0.92 ± 0.11
Combination of two 2-class RFs (aMCI-AD + Normal-aMCI)	0.62 ± 0.25	0.56 ± 0.27	0.57 ± 0.24

The table shows the accuracy, precision, and recall of all classification models

Healthy individuals, aMCI and AD patients can be classified with multiple binary classifiers

Using the indicators of synchronized neural activity as input features, we trained two binary SVM classifiers to separate the three groups of participants. One SVM classifier was trained to classify the normal and aMCI groups, and another to classify the aMCI and AD groups. Linear and nonlinear SVM classifiers were employed to both assess the intrinsic efficacy of the features in separating the groups (linear SVM) and achieve higher performance through the additional classification power yielded through using a kernel (nonlinear SVM).

For the linear SVM classification, the normal-aMCI classifier achieved an accuracy of 0.91 ± 0.11 and the aMCI-AD classifier achieved an accuracy of 0.80 ± 0.19. By combining these two classifiers, we were able to distinguish between the healthy individuals, aMCI and AD patients with an accuracy of 0.64 ± 0.19.

For the nonlinear SVM classification, the normal-aMCI classifier achieved an accuracy of 0.87 ± 0.11 and the aMCI-AD classifier achieved an accuracy of 0.85 ± 0.12. Through combining these two classifiers, we were able to distinguish between the healthy individuals, aMCI and AD patients with an accuracy of 0.73 ± 0.21.

For the random forest classification, the normal-aMCI and the aMCI-AD classifiers achieved accuracies of 0.90 ± 0.20 and 0.90 ± 0.12, respectively. Table 3 shows the detailed performance statistics of the SVM and random forest classifiers.

Discussion and limitations

As dementia is known to disrupt the neural oscillations of the brain, it was not unexpected to observe that the phase and amplitude of gamma oscillations are more synchronized in healthy adults compared to aMCI and AD patients. Our results indicate that phase synchronization is disrupted in both aMCI and AD groups, whereas the amplitude coherence remains unchanged from normal in aMCI patients. This difference may suggest that spatial coherence remains intact in aMCI and offers potential hope for preventing the aMCI state to progress towards AD through early diagnosis and employing interventional therapeutic methods.

PPL

The phase synchronization performance underlying cognitive functions of the brain is disrupted in AD (Knyazeva et al. 2008). The PPL values calculated for the gamma oscillatory band in this study are in agreement with the reported decrease in Global Field Synchronization (GFS) in the alpha, beta, and gamma bands in a study by (Koenig et al. 2005). On the other hand, PPL values are almost identical for the AD and aMCI groups. This indicates that the ability of gamma oscillations in the frontal areas of the brain to maintain a stable phase in time, which is a requirement in cognitive functions such as learning, memory, and perception (Ward 2003), may already be compromised in aMCI patients.

Amplitude coherence

The oscillatory patterns of brain signals are known to be impacted in patients diagnosed with AD in such a fashion that low frequency activity is enhanced and high frequency

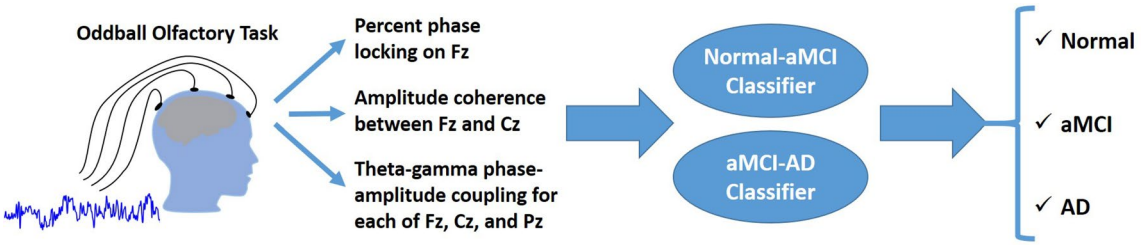

Fig. 4 Flowchart of procedures for classifying the three groups of healthy individuals, and aMCI and AD patients. EEG signal is acquired during an oddball olfactory task and data from 3 electrodes (Fz, Cz, and Pz) are used in the analyses. The features shown in the figure including the PPL, amplitude coherence, and the three theta-gamma PAC values are extracted from EEG data and two binary classifiers are used for normal versus aMCI, and aMCI versus AD classification

oscillations are diminished (Jafari et al. 2020a, b). Our results suggest that the amplitude coherence in high frequencies (gamma band) between the frontal and parietal regions may not be yet as severely damaged in aMCI compared with AD, and the degradations observed in the cognitive functions of aMCI patients may likely be linked to the deficit observed in the phase synchronization of gamma oscillations in the frontal areas as also reported in (Park et al. 2012).

PAC

Theta-gamma PAC has been reported as a brain mechanism involved in working memory functions (Radiske et al. 2020), and its deficit has been reported both in rat AD models and patients diagnosed with AD (Bazzigaluppi et al. 2017). The low values of theta-gamma PAC observed for the AD patients in our study is in alignment with earlier reports (Goodman et al. 2018). The observed increase in the coupling between the theta and gamma oscillatory activity in the aMCI group may be an indication of an attempt by the brain's neuronal networks to maintain regular behavior in face of degradations in the synchronization performance which have started in conjunction with impaired cognitive function (Pusil 2019).

Classification

Given the results observed in this study, we propose a new method that could be potentially used as a topographical biomarker along with other existing diagnosis measures employed by clinicians for diagnosing aMCI and AD. Five indicators of brain synchronization which were introduced earlier are extracted from EEG data acquired during an oddball olfactory task. Based on these indicators, machine learning models can be trained to classify the data of a participant into one of the healthy, aMCI, and AD groups. Classification using the mentioned features offers high accuracy for distinguishing between these groups, which is superior to the classification results reported in (Rallabandi et al. 2020) based on structural MRI data. A flowchart depicting the procedures of the proposed diagnosis method can be seen in Fig. 4.

Our study suggests a new method for differentiating AD and aMCI patients based on a convenient single-session EEG data recording procedure, and offers more accurate results than the classification results reported earlier. This provides a tool that can assist clinicians in distinguishing suspected aMCI cases when other diagnostic criteria do not provide decisive evidence. The proposed passive olfactory-based task is suitable for the elderly who may be unable to take part in active psychophysical or intense cognitive tasks based on visual perception or interpretation. The ability to differentiate aMCI patients from both healthy and AD groups enables the early diagnosis of aMCI, which allows for timely intervention to prevent or decelerate its progress to AD.

Our study had limitations in its scope and implementation in several ways. First, the size of the cohort was limited due to the risks and challenges associated with clinical visits by the elderly during the COVID-19 pandemic. The size of the participant groups hence remained at the minimum required through sample size calculations, limiting our investigation of the efficacy of the proposed topographical markers of aMCI and AD to the scope of a pilot study. Second, the mental states of the participants were diagnosed solely based on clinical representation and cognitive performance in addition to structural MRI data. More extensive CSF or neuroimaging data collection could increase the diagnostic confidence of prodromal Alzheimer's disease as well as reveal the correlation between the proposed network-level indicators of synchronization quality and the underlying mechanisms of the progression of aMCI towards AD, and should be considered in the design of future studies. Third, our study was based on a cross-sectional comparison of the three participant groups while a longitudinal study is required to draw conclusions on how the proposed synchronization indicators evolve over time for the aMCI and AD patients as their status progresses

to other stages of the disease. Fourth, we reported results based on analyzing data from a limited number of channels chosen according to earlier reports. A more extensive analysis using data of all channels and performing graph-based analysis could reveal additional insight into the topographical spread of oscillatory deficits across the brain and lead to better diagnosis performance. Due to the mentioned limitations, the observations and deductions made in this article should be construed as preliminary. Despite these limitations, our observations provide hints towards a potentially interesting direction for a more extensive evaluation of the network-level changes involved in the progression of amnestic MCI to Alzheimer's disease.

Acknowledgements The authors wish to thank Ziaeian Hospital in Tehran for providing staff time and equipment for data collection in this study. We are grateful to the patients and their families who participated in this study.

Author contributions HA conceptualized the work. MJS and HA designed the experiments. MJS and ZV collected the data. MJS, SNF, and AA analyzed the data. MJS, SNF, AA, and HA wrote the manuscript. HA and ZV supervised the work. All authors edited and approved the manuscript.

Funding This work was partially funded by the Cognitive Sciences and Technologies Council of Iran and by the Grant G970736 from Sharif University of Technology, which covered the cost of data collection. The funders had no role in the study conceptualization and design, data collection and analysis, decision to publish, or preparation of the manuscript. The authors have no other competing interests to declare that are relevant to the content of this article.

Data availability statement Access to the data used to derive the results of this study will be provided upon reasonable request.

Declarations

Conflict of interest The authors have not disclosed any competing interests.

Compliance with ethical standards This study was approved by the Review Board of Tehran University of Medical Sciences (Approval ID: IR.TUMS.MEDICINE.REC.1398.524). All methods were performed in accordance with the relevant guidelines and regulations and the ethical standards in the Declaration of Helsinki. All participants gave their written consent before beginning the experiment and were free to withdraw at any time. The name and date of birth of the participants were kept confidential and were not used in any of the analyses.

References

Akiyoshi R (2018) Microglia enhance synapse activity to promote local network synchronization. eNeuro 5(5)

Albert M et al (2011) The diagnosis of mild cognitive impairment due to alzheimer's disease: recommendations from the national institute on aging-alzheimer's association workgroups on diagnostic guidelines for Alzheimer's disease. Alzheimer's Dement. 7(3):270–279

Aron L, Yankner BA (2016) Neural synchronization in Alzheimer's disease. Nature 540(7632):207–208

Augusto-Oliveira M et al (2019) What do microglia really do in healthy adult brain? Cells 8:1293

Babiloni C et al (2020) Abnormal cortical neural synchronization mechanisms in quiet wakefulness are related to motor deficits, cognitive symptoms, and visual hallucinations in parkinson's disease patients: an electroencephalographic study. Neurobiol Aging 91:88–111

Güntekin B, Saatçi E, Yener G (2008) Decrease of evoked delta, theta and alpha coherences in Alzheimer patients during a visual oddball paradigm. Brain Res 1235:109–116

Balbi M et al (2021) Gamma frequency activation of inhibitory neurons in the acute phase after stroke attenuates vascular and behavioral dysfunction. Cell 34:108696

Bazzigaluppi P et al (2017) Early-stage attenuation of phase-amplitude coupling in the hippocampus and medial prefrontal cortex in a transgenic rat model of Alzheimer's disease. Hum Brain Mapp 144:669

Bell A, Sejnowski T (1995) An information-maximization approach to blind separation and blind deconvolution. Neural Comput 7:1129

Bonnefond M. Kastner S Jensen O (2017) Communication between brain areas based on nested oscillations. eNeuro 4(2)

Bouyer J, Montaron M, Rougeul A (1981) Fast fronto-parietal rhythms during combined focused attentive behaviour and immobility in cat: cortical and thalamic localizations. Electroencephalogr Clin Neurophysiol 51:244

Caravaglios G, Castro G, Costanzo E (2010) Theta power responses in mild Alzheimer's disease during an auditory oddball paradigm: lack of theta enhancement during stimulus processing. J Neural Transm 117:1195–1208

Delorme A, Makeig S (2004) EEGLAB: an open-source toolbox for analysis of single-trial EEG dynamics. J Neurosci Methods 134:9–21

Devanand D et al (2000) Olfactory deficits in patients with mild cognitive impairment predict Alzheimer's disease at follow-up. Am J Psychiatry 157(9):1399–1405

Dimitriadis SI et al (2015) A novel biomarker of amnestic MCI based on dynamic cross-frequency coupling patterns during cognitive brain responses. Front Neurosci 9:350

Dubois B et al (2014) Advancing research diagnostic criteria for Alzheimer's disease: the IWG-2 criteria. Lancet Neurol 13(6):614–629

Galloway DA, Phillips AE, Owen DR, Moore CS (2019) Phagocytosis in the brain: homeostasis and disease. Front Immunol 16:790

Goodman MS et al (2018) Theta-gamma coupling and working memory in alzheimer's dementia and mild cognitive impairment. Front Aging Neurosci 10:101

Hahn E, Andel R (2011) Nonpharmacological therapies for behavioral and cognitive symptoms of mild cognitive impairment. J Aging Health 23(8):1223–1245

Henao D, Navarrete M, Valderrama M (2020) Entrainment and synchronization of brain oscillations to auditory stimulations. Neurosci Res 156:271–278

Hojjati H et al (2019) An inexpensive and portable olfactometer for event-related potential experiments. In: IEEE Austria international biomedical engineering conference Vienna

Iaccarino H et al (2016) Gamma frequency entrainment attenuates amyloid load and modifies microglia. Nature 540(7630):230–235

Jafari Z, Kolb BE, Mohajerani MH (2020a) Neural oscillations and brain stimulation in Alzheimer's disease. Prog Neurobiol 194:101878

Jafari Z, Kolb B, Mohajerani M (2020b) Neural oscillations and brain stimulation in Alzheimer's disease. Prog Neurobiol 194:101878

Jebelli J, Su W, Hopkins S, Pocock J, Garden GA (2015) Glia: guardians, gluttons, or guides for the maintenance of neuronal connectivity?. Ann N Y Acad Sci 1351(1):1–10

Jia X, Smith M, Kohn A (2011) Stimulus selectivity and spatial coherence ofgamma components of the local field potential. J Neurosci 31(25):9390–9403

Jungwirth S et al (2012) The validity of amnestic MCI and non-amnestic MCI at age 75 in the prediction of Alzheimer's dementia and vascular dementia. Int Psychogeriatr 24(6):959–966

Kay LM (2015) Olfactory system oscillations across phyla. Curr Opin Neurobiol 31:141–147

Kleen JK et al (2016) Oscillation phase locking and late erp components of intracranial hippocampal recordings correlate to patient performance in a working memory task. Front Hum Neurosci 10:287

Knyazeva MG et al (2008) Topography of EEG multivariate phase synchronization in early Alzheimer's Disease. Neurobiol Aging 37(7):1132–1144

Knyazeva MG, Carmeli C, Khadivi A (2012) Evolution of EEG synchronization in early Alzheimer's disease. Neurobiol Aging 34(3):694–703

Koenig T et al (2005) Decreased EEG synchronization in Alzheimer's disease and Mild cognitive impairment. Neurobiol Aging 26(2):165–171

Kramer MA et al (2007) Synchronization measures of the scalp electroencephalogram can discriminate healthy from alzheimer's subjects. Int J Neural Syst 17(2):61–69

Le Van Quyen M et al (2001) Comparison of Hilbert transform and wavelet methods for the analysis of neuronal synchrony. J Neurosci Methods 111(2):83–98

Lee D, Landreth G (2010) The role of microglia in amyloid clearance from the AD brain. Basic Neurosci Genet Immunol 117(8):949–960

Lega B, Burke J, Jacobs J, Kahana MJ (2014) Slow-theta-to-gamma phase-amplitude coupling in human hippocampus supports the formation of new episodic memories. Cereb Cortex 26(1):268–278

Liang Z, Bai Y, Ren Y, Li X (2016) Synchronization measures in eeg signals. Signal Process Neurosci 167:202

Liu Y et al (2021) Microglia elimination increases neural circuit connectivity and activity in adult mouse cortex. J Neurosci 41(6):1274–1287

Mattsson N, Palmqvist.Stomrud SE et al (2019) Staging β-amyloid pathology with amyloid positron emission tomography. JAMA Neurol 76(11):1319–1329

Mesholam RI, Moberg PJ, Mahr RN, Doty RL (1998) Olfaction in neurodegenerative disease. A meta-analysis of olfactory functioning in Alzheimer's disease and Parkinson's disease. Arch Neurol 55:84–90

Montaron M-F, Bouyer J-J, Rougeul A, Buser P (1982) Ventral mesencephalic tegmentum (VMT) controls electrocortical beta rhythms and associated attentive behaviour in the cat. Behav Brain Res 6(2):129–145

Morgan CD, Murphy C (2002) Olfactory event-related potentials in Alzheimer's disease. J Int Neuropsychol Soc 8:753–763

Mouly AM, Sullivan R (2010) Memory and plasticity in the olfactory system: from infancy to adulthood. In: Menini A (ed) The neurobiology of olfaction. CRC Press/Taylor & Francis, Boca Raton (FL). Chapter 15. Available from: https://www.ncbi.nlm.nih.gov/books/NBK55967/

Munia TTK, Aviyente S (2019a) Comparison of wavelet and ridrihaczek based methods for phase-amplitude coupling. IEEE 26:1897–1901

Munia TTK, Aviyente S (2019b) Time-frequency based phase-amplitude coupling measure for neuronal oscillations. Sci Rep 9(1):1–15

Park J et al (2012) Gamma oscillatory activity in relation to memory ability in older adults. Int J Psychophysiol 86(1):58–65

Pedregosa F et al (2011) Scikit-learn: machine learning in python. J Mach Learn Res 12:2825–2830

Petersen RC (2016) Mild cognitive impairment. Continuum (Minneap Minn) 404–418. https://doi.org/10.1212/CON.0000000000000313

Poza J et al (2017) Phase-amplitude coupling analysis of spontaneous EEG activity in Alzheimer's disease. IEEE. https://doi.org/10.1109/EMBC.2017.8037305

Pusil S et al (2019) Hypersynchronization in mild cognitive impairment: the "X" model. Brain 142(12):3936–3950

Quiñones-Camacho LE et al (2021) Dysfunction in interpersonal neural synchronization as a mechanism for social impairment in autism spectrum disorder. Autism Res 14(8):1585–1596

Radiske A et al (2020) Cross-frequency phase-amplitude coupling between hippocampal theta and gamma oscillations during recall destabilizes memory and renders it susceptible to reconsolidation disruption. J Neurosci 40(33):6398–6408

Rallabandi VS, Tulpule K, Gattu M et al (2020) Automatic classification of cognitively normal, mild cognitive impairment and Alzheimer's disease using structural MRI analysis. Info Med Unlocked 18:100305

Reinhart RM, Nguyen JA (2019) Working memory revived in older adults by synchronizing rhythmic brain circuits. Nat Neurosci 22(5):820–827

Rubino D, Robbins KA, Hatsopoulos NG et al (2006) Proagating waves mediate information transfer in the motor cortex. Nat Neurosci 9:1549–1557

Sedghizadeh MJ et al (2020) Olfactory response as a marker for Alzheimer's disease: evidence from perceptual and frontal lobe oscillation coherence deficit. PLoS ONE 15(12):e0243535

Silva M, Mercer P, Witt M, Pessoa R et al (2018) Olfactory dysfunction in alzheimer's disease systematic review and meta-analysis. Dement Neuropsychol 12:123–132

Srinath R, Ray S (2014) Effect of amplitude correlations on coherence in the local field potential. J Neurophysiol 112(4):741–751

Talamo BR et al (1989) Pathological changes in olfactory neurons in patients with Alzheimer's disease. Nature 337:736–739

Tass PA, Rosenblum M, Weule J et al (1998) Detection of n:m phase locking from noisy data: application to magnetoencephalography. Phys Rev Lett 81:3291

Timofeev I, Bazhenov M, Seigneur J et al (2012) Neuronal synchronization and thalamocortical rhythms in sleep, wake and epilepsy. In: Noebels JL, Avoli M, Rogawski MA et al (eds) Jasper's basic mechanisms of the epilepsies [Internet], 4th edn. National Center for Biotechnology Information (US), Bethesda (MD). Available from: https://www.ncbi.nlm.nih.gov/books/NBK98144/

Valencia AL, Froese T (2020) What binds us? inter-brain neural synchronization and its implications for theories of human consciousness. Neurosci Conscious 2020(1):niaa010. https://doi.org/10.1093/nc/niaa010

Wang Z et al (2019) Functional connectivity changes across the spectrum of subjective cognitive decline, amnestic mild cognitive impairment and Alzheimer's disease. Front Neuroinform. https://doi.org/10.3389/fnagi.2022.879836

Ward LM (2003) Synchronous neural oscillations and cognitive processes. Trends Cogn Sci 7(12):553–559

Womelsdorf T, Fries P (2007) The role of neuronal synchronization in selective attention. Curr Opin Neurobiol 17(2):154–160

Yener G, Güntekin B, Oniz A, Başar E (2007) Increased frontal phase-locking of event-related theta oscillations in Alzheimer patients treated with cholinesterase inhibitors. Int J Psychophysiol 64(1):46–52

Zhan Y et al (2014) Deficient neuron-microglia signaling results in impaired functional brain connectivity and social behavior. Nat Neurosci 17:400–406

Zhao J, Du Y-Z, Ding X-T et al (2020) Alteration of functional connectivity in patients with Alzheimer's disease revealed by resting-state functional magnetic resonance imaging. Neural Regen Res 15(12):285–292

Zou Y et al (2016) Olfactory dysfunction in Alzheimer's disease. Neuropsychiatr Dis Treat 12:869